Assessment of Landslide Event in Naltar Valley, Gilgit-Baltistan, Pakistan using Optical Imagery

Rana, A. S.[1,2], N. Hussain[2], M. Haroon[2]

Abstract

A catastrophic mass flow including ice, debris and water sprung from the upstream of Naltar valley, Gilgit on 5th July 2021 causing devastation to Naltar forest and blocking the passage of Naltar river few hundred meters below the Satrangi lakes forming temporary lakes (two in numbers) covering an area of about 0.02 km^2 and 0.04 km^2 respectively. After the event 4 persons including two women were reported to be missing due to the catastrophe. We use satellite imagery of pre and post disaster period to assess the situation and figured out the reasons of the disaster. 12.5 meter spatial resolution Digital Elevation Model (DEM) was also used to trace the slope and path of the sliding event. A rock slab with an area of approximately 56153 m^2 was detached from the steep slope of the mountain and triggered a mass movement which collapsed the ablation area and snout of the adjoining glacier. A scar can be clearly seen at the upstream of detached slab which is joined with the accumulation region of hanging glacier of adjacent nullah. Permafrost thaw process and different lithology of rocks could have triggered this scar. Almost 1.2 km^2 area below the detached location was effected creating small scale flood in Naltar valley. The debris including small and large boulders and morainic material finally accumulated at the foot of the mountain and devastated 0.32 km^2 forest area. The landslide susceptibility map highlighting vulnerable locations needs to be assessed for rapid response activities in case of disaster. The antecedent conditions and immediate societal response will allow for sustainable development in remote mountainous areas, immediate mitigative measures and developing resilient communities.

Key words: Mass movement, Naltar, DEM, Satellite imagery.

Introduction

Mass movements like debris flow, landslides and avalanches are influenced by natural and anthropogenic factors (Chen et al., 2015). It is one of the most important and frequent geomorphological hazard which poses significant physical and environmental threat to communities in mountainous areas (Gong et al., 2021). It is estimated that almost 2.5% of world's land surface is prone to landslides and almost 5% of the world population are exposed to this hazard (Dilley et al., 2005). Every year thousands of casualties, loss of livestock, infrastructure and agricultural lands occur due to these hazards throughout the world (Papathoma-Köhle et al., 2007; Feizizadeh and Blaschke, 2011). Therefore, the identification of potential mass movement locations, monitoring and control measures are necessary for policy makers and planers to prevent or minimize the losses (Pradhan et al., 2011). Mass movements can be triggered by diversity of external factors and stimuli (Wieczorek, 1996) which vary from region to region, however, high topographic relief, seismic activity, intense or prolonged rain and human interventions are considered most widespread globally (Keefer, 2002; Guzzetti et al., 2008). In terms of magnitude seismicity induced slides are most disastrous (Bouhadad et al., 2010) and seismic events are one of the largest triggers of mass movement. Almost 1293 landslides were identified at 174 locations in Balakot alone after 2005 earthquake in Kashmir valley (Owen et al., 2008). Apart from seismic induced slides, rainfall triggered mass movements also have highest frequency of occurrences (Li et al., 2010). Most of the mass movements could be triggered by a combination of causative factors mentioned above.

Many statistical, qualitative, quantitative, and machine learning approaches have been developed to assess the mass movements due to recent advances of computer processing coupled with information systems and

[1] adnanshafiqrana@gmail.com
[2] Pakistan Meteorological Department

remote sensing (Wang et al., 2013; Tien Bui et al., 2016; Zhang et al., 2016; Tsangaratos et al., 2017). These recent advances incorporating satellite information with in-situ measurements has made possible to detect the reasons of mass movements along with its proper assessment and guidelines for future. These advances also helps in the generation of detailed relevant data required for assessment and recently many numerical modeling techniques have been developed for better understanding of such events (Zhuang et al., 2020; Abraham et al., 2021). The advent of high resolution optical remote sensing data has greatly enhanced our abilities to monitor mass movements taking advantage over traditional ground instrumentation. This technique can cover large area and generation of continuous data geographically instead of point data collected by in-situ measurements. However expertise in analyzing these images and extract useful information needs expertise on image interpretation and processing. Further, the development of database of mass movements can be very valuable source in which information for research is available, mentioning the reasons, types, processes, impacts, indigenous knowledge about sliding events (Hurst et al., 2013) but unfortunately no such database exist for events reported in Pakistan.

Despite awareness about mass movements and advancements in testing, modeling, risk assessment with prior knowledge about mass movement, its location, probable timings (Mikoš et al., 2017), yet natural phenomenon can't be stopped or reverted. Every year lot of such incidents occur claiming hundreds of thousands lives and material losses. One of the greatest disaster occurred in Tadzhikistan in 1949 when series of mass movements occurred due to earthquake of magnitude 7.5, resultantly buried 33 villages and death toll of around 12000 to 20000 people (Wesson and Wesson, 1975). The landslide near Oso, Washington along the North Fork of Stillaguamich river in Snohomish Country on 22nd March 2014 is considered deadliest in the history of U.S. with 43 casualties (Wartman et al., 2016). A catastrophic mass flow that descended from high valley flanks of Rishiganga and Dhaulinganga in Chamoli, Uttrakhand, India in February 2021 killed over 200 people (Shugar et al., 2021). Having complex arduous terrain and diverse landscape, mass movements are also very frequent and recurrent phenomenon in the mountainous regions of Pakistan (Schneider et al., 2013; Pandey et al., 2021) in which the Himalayan region is the worst slide hit region (Kazmi., A.H and Jam., 1997; Saha et al., 2005). The regions with good precipitation events are more prone to landslides and rock avalanches for example lesser Himalayas in Pakistan with highest average annual rainfall during monsoon season are the worst landslide hit areas. The mountains in northern Pakistan are also susceptible to landslides and mass movements which can be triggered even after small-scale precipitation event. One of the renowned landslide event occurred at Attabad Hunza in 2010 which result in the formation of Attabad lake covering a maximum area of almost 8.3 km^2 as calculated using satellite image of 2011 which has now been reduced to 4.12 km^2 This lake remained a continuous nuisance for the lives of the local people cutting road access between upper Hunza and rest of Pakistan until construction of new road in September 2015.

The mass movements may also result in the formation of impounded lakes whose volume vary significantly from several hundred cubic meters to several cubic kilometers and poses another kind of threat to the mountainous communities (Evans et al., 2011) due to their various levels of de-stability. The Usoi dam is known to be the world's largest rock slide impounded reservoir on earth in Tajikistan with a volume of almost 16 km^3 (Ischuk, 2011). These dams formed due to mass movements may outburst/ breached resulting in flood episode with debris flow and devastate large areas displacing large number of vulnerable communities. A dam breach along Dadu river in Sichuan, China claimed thousands of lives which was formed as a result of landslide triggered by an earthquake of 7.7 magnitude (Dai et al., 2005). One of the largest earthquake-triggered landslide was occurred near Nanga Parbat, Pakistan in December 1840 to January 1841 and impounded 30 km long lake with approximate depth of 150 meters which outburst in June 1841 releasing 3-5 billion cubic meter of water (Shroder, 1998; NESPAK, 2010). Another slope failure landslide occurred in 1858 near Sulmanabad just downstream of Attabad blocking Hunza river (Shroder, 1998). Thousands of mass movement events occurred in last 50 years albeit many gone unreported. Among them few of the recent reported events include Khurdopin glacier surge in 1979, 2000 and 2017 (Quincey and Luckman, 2014; Steiner et al., 2018), Hattian Bala in 2005, Attabad in 2010 (Schneider et al., 2013), Shishper glacier in 2018 (Khan et al., 2021), and Badswat in 2017 (Shangguan et al., 2021) and 2021.

The landslide and rock avalanche events in snow and glaciated region are, therefore, more hazardous due to the sensitivity of snow, ice and permafrost to climate change (Fischer et al., 2012; Gruber et al., 2017). In such areas hazard cascades initialized by snow, ice or rock slide and the area remain under disaster for longer interval (Shangguan et al., 2021; Shugar et al., 2021). Global warming rapidly cause melting of glacial ice in recent era and resultantly, glacier hazards increased in magnitude and frequency. A rock avalanche occurred in Naltar Valley on 5th July 2021 damaging forest in Naltar Valley and claiming 4 lives including two women as per local news respondents (Dawn, 2021) and National Disaster Management Authority (NDMA), Pakistan. This paper discusses about the position and shape of the sliding surface, possible cause of the slide, approximate volume of debris accumulated due to sliding activity, land degradation and ecosystem loss and further prevailing hazard due to slide using satellite imagery and Digital Elevation Model of the area.

Study Area

Naltar Valley is one of the renowned valley located at a distance of 34 kilometers from Gilgit (Figure 1). The landscape of the valley is characterised by alpine relief with steep slopes and U shaped glacial valleys/gullies located along the main Naltar river stream. The valley is located in between Main Karakoram Thrust (MKT) and Main Mantle Thrust (MMT). The valley catchment covers an area of 273.7 km^2 and its main river stream originates from the snout of Shani glacier at an elevation of approximately 4500 meters above sea level (m.a.s.l.) and after covering a distance of 32 km falls in Hunza river (Figure 2). The Naltar pass connects Naltar Valley with Pakora valley in Ishkomen, Ghizer. There are 50 small and large glaciers in the valley covering an area of 30.3 km^2 The largest glacier is Shani glacier located at Naltar pass with an area of 12.9 km^2 There are 9 lakes in the valley among which three tourist attraction lakes are Satrangi lake, Blue lake and Bodlok lake. These lakes are not considered as potentially dangerous lake. Naltar is also a forested region known for its greenish mountain scenery. Naltar Bala (upper) and Naltar Paain (lower) are two main villages of Naltar valley. The incident occur in a Nullah (valley) just downstream from Satrangi, Blue and Bodlok lakes and debris mass separates from an elevation of almost 4700 m.a.s.l.

Data and Methodology

We used ALOS-PALSAR Radiometrically Terrain Corrected (RTC) Digital Elevation Model (DEM) from Alaska Satellite Facility (ASF) at 12.5 meter spatial resolution downloaded from Distributed Active Archive Center (DAAC) (Dataset: ASF DAAC, 2015)to delineation of Naltar catchment, extract slope and curvature of sliding area and drainage networks for performing morphometric analysis. Further the satellite images acquired by Sentinel optical imaging satellite before and after the event was used to perform the assessment of land sliding location (Table 1). Sentinel optical imaging satellites for observing the earth was launched as a part of European Space Agency Copernicus Program in 2015 aboard Multi Spectral Instruments (MSI) having 13 spectral bands with spatial resolution of 10 meters (four visible and near-infrared bands), 20 meters (six red edge and shortwave infrared bands) and 60 meters (three atmospheric correction bands).

Results and Discussion

A flood hit the valley on 5th July 2021 as per local respondents and district disaster management authority. The local people were of the view that there was a glacier surge episode which blocked the river and resultantly, a lake was formed. But as per assessment of post and pre disaster satellite images it is clear that there was a rock slide which also erodes the ice of the glacier in the vicinity, snow residue of previous season (Figure 3 and 4). The detached and eroded mass accumulates on the main river flow, blocks the river and results in the formation of lake. The size of the lake was 0.135 km^2 as per satellite image acquired on 9th July 2021 (Figure 3 and 4) which has been reduced/ increased to 0.075 km^2 as per satellite imagery acquired on 5th April 2022. Generally 80% of these mass movement impounded dams failures occur in the first year of its formation (Costa and Schuster, 1988; Ermini and Casagli, 2003; Evans et al., 2011), however, the lake formed as a result of this landslide is still intact. The eroded snow and ice impacted the

mountain floor and thus frictional heating also triggered flood wave which was observed by the local community residing downstream of the incident location.

Table 1: List of Satellite images used for geomorphic mapping in this study.

Pre-Event				
S. No.	**Sensors/ Source**	**Path/ Row**	**Image Acquisition Date**	**Resolution (meters)**
1	Sentinel-2 Multispectral Instrument	T43SDA	23-08-2020	10
2	Sentinel-2 Multispectral Instrument	T43SDA	22-09-2020	10
3	Sentinel-2 Multispectral Instrument	T43SDA	04-06-2021	10
4	Sentinel-2 Multispectral Instrument	T43SDA	09-06-2021	10
5	Sentinel-2 Multispectral Instrument	T43SDA	24-06-2021	10
6	Google Earth Image		10-07-2017	
7	ALOS DEM	528/ Frame 710	06-03-2008	12.5
Post Event				
8	Sentinel-2 Multispectral Instrument	T43SDA	09-07-2021	10
8	ASTER	14/ 209	12-07-2021	15
9	Sentinel-2 Multispectral Instrument	T43SDA	24-07-2021	10
10	Sentinel-2 Multispectral Instrument	T43SDA	27-09-2021	10

An area of 0.056 km^2 of rock and debris was detached from the mountain flanks at an elevation range of 4344 m.a.s.l. to almost 4683 m.a.s.l. effecting almost 1.2 km^2 area in which 0.2 km^2 area consists of rock glacier (Figure 4). The landslide path and triggering location of the event identified by Gardezi et al., (2022) is not correct as per investigations done in this study. This detached mass separated on the basis of visual interpretation of satellite images (Table 1) acquired after landslide event is smaller than the slab detached from Ronti Peak in Chamoli, Uttrakhand, India incident (Shugar et al., 2021) and Badswat, Pakistan incident of 2017 (Shangguan et al., 2021), both of which triggers cascade of events. Thus the magnitude of destruction is smaller than the Uttrakhand incident but can be comparable to Badswat incident in terms of land degradation. The land slide initiation location shows a different lithology from the surroundings and a scar with cracks are also visible at the top of the sliding detached slab at an elevation of 4700 m.a.s.l. as per google image (Figure 5 and 6). These cracks may results from the thaw process of permafrost coupled with differentiation in rock/ soil type and lithology. The slope gradient of detached part lies between 2° and 64° having frequency of 51% in the interval 20° to 51° and 27% greater than 51° slope (Figure 7 and 8). The slopes gradients between these interval are highly susceptible for triggering significant landslides (Klose et al., 2014) in addition to lithological properties and other characteristics. Further the slope curvature of the detached part is combination of convexity and concavity with high frequency of convexity which increased the probability of high landslide susceptibility. Unfortunately, the volume of detached part couldn't be figured out accurately mainly due to nonavailability of pre and post disaster DEM. However it is estimated that the average depth of the detached part is 7 meters calculated using google earth image showing crack width within rock of different lithology (Figure 5 and 6). Thus based on this average depth the total volume of 0.0004 km^3 was detached and slipped downward all the way to the elevation of 3200 m.a.s.l. The debris flow that initiates from an elevation of 4700 m.a.s.l. approximately covers a distance of 3.6 kilometers

below to the location of accumulation at almost 3200 m.a.s.l. (Figure 7). The flow path slightly bends at an elevation interval of 3900-4000 m.a.s.l. (Figure 4). The slope shows that the sliding flow path is very steep (Figure 8) and, therefore, we can argued that the velocity of this slide will be exceptionally high as compared to other landslides events (Shangguan et al., 2021; Shugar et al., 2021).

While sliding at exceptionally high pace, the detached patch also erodes layer of debris, snow and ice along its flow path, finally accumulates over the Naltar river blocking it and results in the formation of erosion lake. The fresh trace visualized in the image of 9th July 2021 i.e. immediately after slide shows that the mass movement erode the ice of glacier and causes it to collapse from the ablation zone and snout (Figure 4). It also washes all the snow on its way that was still prevailing and not melted from the last snow season (Figure 3). The exposed ice of a debris covered rock glacier clearly indicate that 0.22 km^2 of glacier area was effected and if we assumes that it erodes averagely 1 meter of the glaciated ice then its 0.0002 km^3 volume slides with the mass movement which finally melts due to frictional pressure of landslide event and heat at lower elevations. The total area including the glaciated part that was effected due to passage of mass movement constitutes to 1.17 km^2 It is also observed that a small meagre slide also travels towards the northern aspect of the cliff triggering landslide (Figure 9) which contradicts the origin of slide detected by (Gardezi et al., 2022). It is difficult to estimate the accurate depth of eroded part at the southern aspect of slide in the absence of field data and nonavailability of pre and posts disaster elevation data. If we consider the average depth of eroded surface to be 12 meter from the study done by (Gardezi et al., 2022), then the total volume which was accumulated as fluvial fan is almost 0.015 km^3, which is almost half of rock and ice detached from Ronit Peak (Shugar et al., 2021) and is in agreement with the magnitude of disaster in two cases. Additionally it could be argued that damage of the forest just below the glacier snout having tall trees at small inclined locations from its surroundings along the flow path (Figure 10) gives an insight that eroded apart at this location is not less than 8 meters based on difference of elevations (Figure 11).

The detached debris and eroded part due to mass movement splits into two paths due to topographic differences and water flow path already defined. The inclined locations of forest area located at upper flanks of valley floor forms the basis for division of mass movement flow (Figure 11). The two parts of mass movements damage the forest area on their way and finally accumulates over the Naltar river flow blocking river and a lake was formed (Figure 3 and 4). The depth of the alluvial fan deposited at low elevations is different at different elevations and couldn't be estimated accurately. The total area of accumulated alluvial fan is almost 0.26 km^2 consisting of upper portion and lower part having areas 0.07 km^2 and 0.19 km^2 respectively (Figure 4). The slide also effects the forest at the foothill of the sliding area and damaged almost 0.32 $km^2$of forest area (Figure 3). The lake formed due to sliding needs to be drained in a controlled way in order to avoid any possible lake outburst event and possible devastation.

An implication of a fractal grain-size distribution and its accumulation blocking the Naltar River may trigger a small scale flash flood event in future. It may be a coarse carapace overlying a very much finer interior. This raised the possibility that if the overflow channel were eroded through the carapace, it might encounter more erodible materials, perhaps leading to rapid breaching of the dam.

Conclusion

Initially the local people informed about the flood event in Naltar valley on 5th July 2021, however, our assessment concludes that it was rock avalanche collapsing glacier snout and side moraine forming a lake by blocking Naltar River. Despite many limitations of assessment due to high sensitivity of approaches for estimation of detached part, its volume, eroded part and accumulated alluvial fan, quality of input data in terms of available satellite imagery and topographic relief data influencing quality of results, yet the assessment provides in insight about the triggering mechanisms of the slide, possible impacts and future implications. The steep slopes, high topographic relief and fissures within rock of different type could trigger rock slide and later on snow and ice erosions, however, exact reason is could be different. There might be remnants of permafrost in the rock slide location whose thaw process could have triggered the

rock slide or the slide area may consists of loose material. A continued monitoring of lake and situation of area is needed to effectively manage the situation in case the lake breaches. The risk of Lake Outburst flood still persists whose probability will increase in summers of the year 2022. There is a need to assess the condition of damming walls and to assess the probability of further sliding in the disaster hit area by visiting the location with surveying equipment like Differential GPS and surveying theodolites.

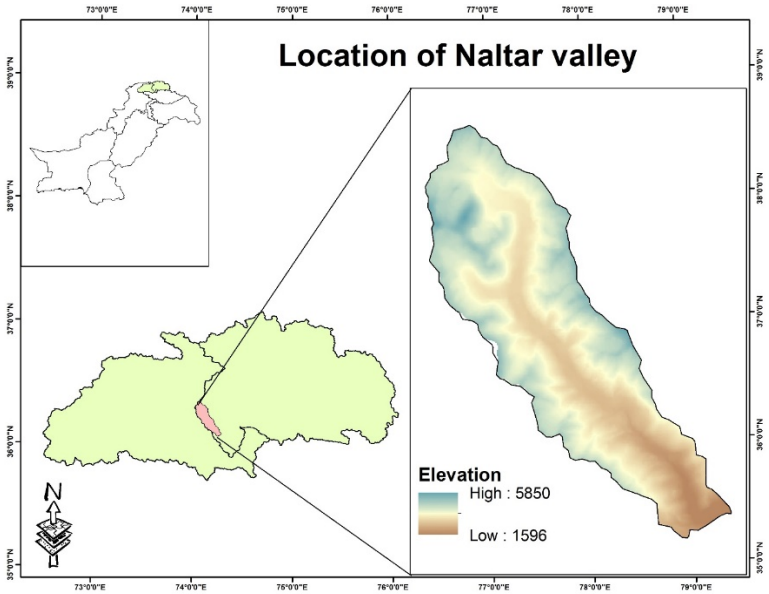

Figure 1: Location of Naltar Valley in Gilgit-Baltistan. It is located in the center of Gilgit Catchment and at the boundary of Hunza river basin. The Naltar river falls in Hunza river which ultimately drains in Gilgit river.

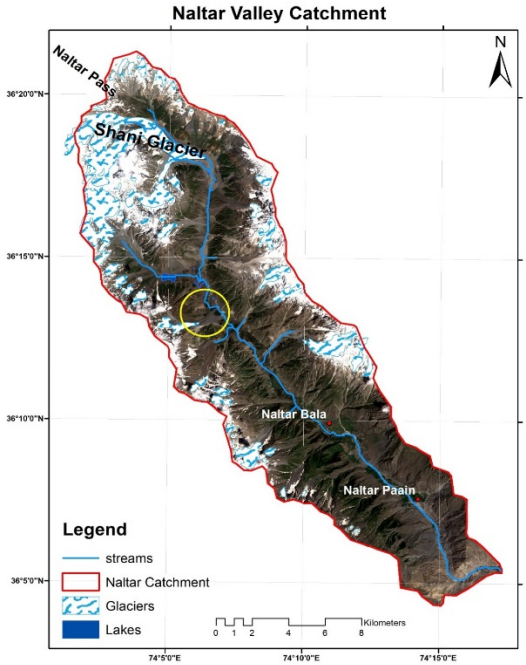

Figure 2: Naltar Catchment area. Shani glacier is the largest glacier situated in the north of the catchment from where the main river stream of Naltar valley originates and falls in Hunza river. Yellow circle shows the location of slide ridge and effected glacier. The location of two main villages of Naltar area also shown.

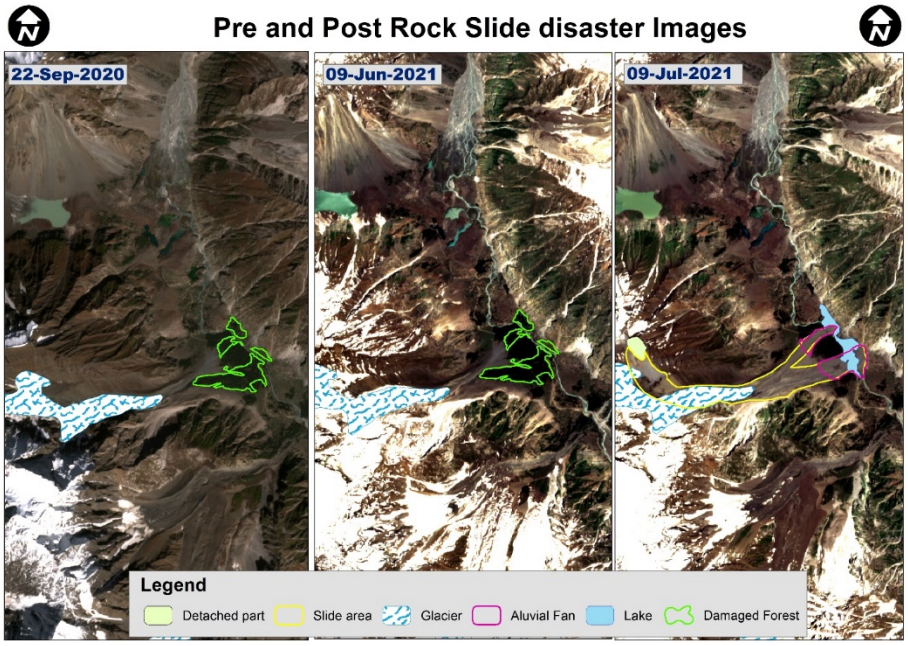

Figure 3: The maps showing the comparison of Naltar area before and after rock slide disaster event. The rock slide triggers from the location shown in light green polygon. Full view of post disaster image is shown in Figure 4. The yellow line show the extent of effected area from where the debris mass slides. The glaciated area which was effected due to slide is also visible. The slide results in accumulation of alluvial fan at the valley floor which block the Naltar river flow and a lake forms resultantly (blue polygon). The damaged portion of forest in the downstream of glacier can also be seen. The presence of snow from last accumulation season is also visible on satellite image acquired on 9th June 2021. The snow was also present in the later image acquired on 24th June 2021 but the detach part was covered with clouds.

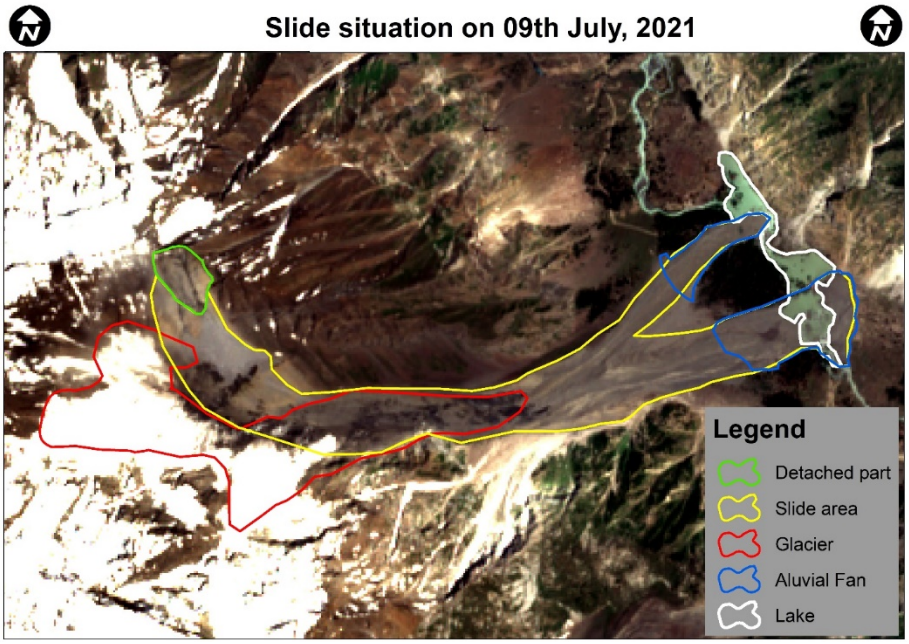

Figure 4: The pictorial view of detached part, landslide flow path, accumulated alluvial fan and glaciated region effected by slide flow debris. These were delineated using post slide images of different times mentioned in Table 1, however, the satellite image acquired on 9th July 2021 was placed below these polygons for visualization. The damage to the glacier is clear exposing glacier ice after erosion of debris which was lying over glacier before event. A small slip in glacier ice is also visible which is lying outside glacier polygon. Fresh piles of dust and debris are clearly visible at the southern side of debris flow path which have been cleared in later images. The sliding flow path bands near the elevation band of 3900-4000 m.a.s.l. (from black cross-sectional line) and later on divides into two parts at lower elevations.

Figure 5: The red polygon is the slab that was detached and slides down eroding the flow path which finally accumulates at valley beds over Naltar river. The yellow lines show the estimated depth of slab from the crack to the surface of the slab part. The zoomed-in snap of this part is shown in Figure 6.

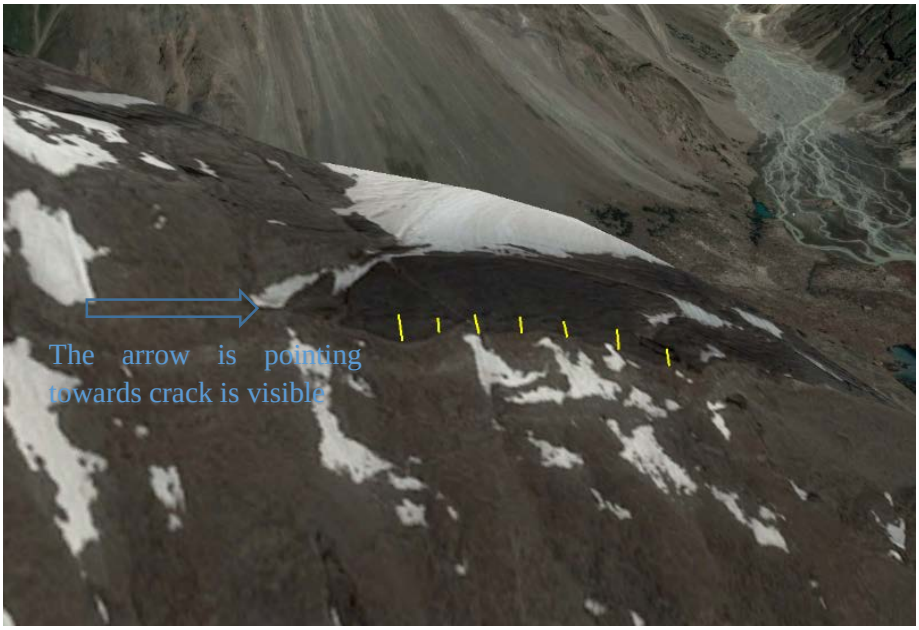

Figure 6: The fissure and fractures are very clear in the rock of different texture and lithology from where the Naltar landslide triggers.

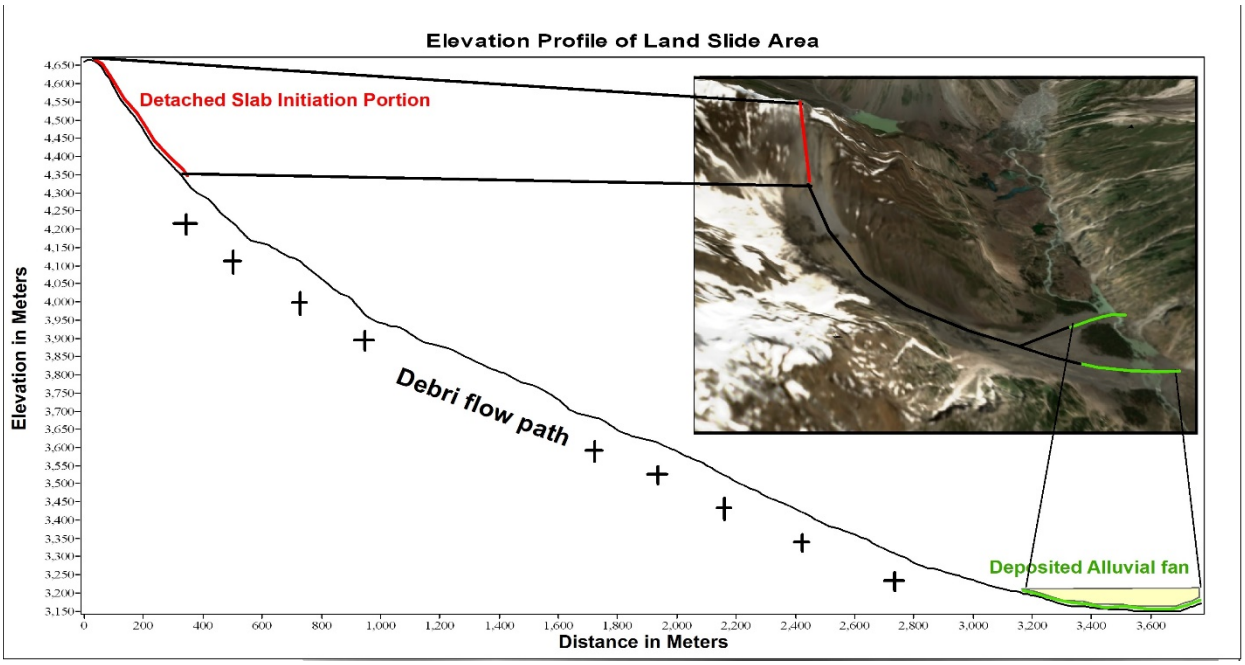

Figure 7: The elevation gradient of detached part, travel path of mass movement and accumulated alluvial fan.

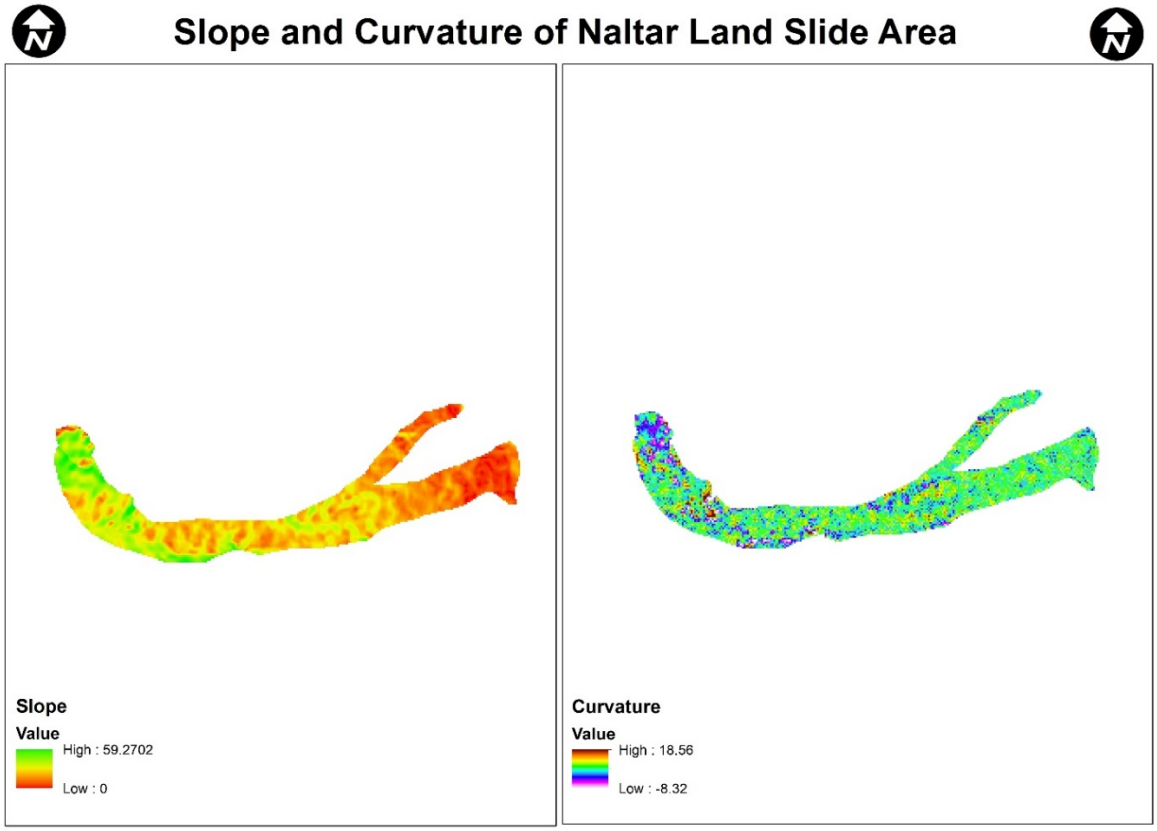

Figure 8: The slope and curvature of sliding flow path. The steep slope and high frequency of convexity at higher elevations elaborates the high velocity of sliding mass which accumulates at lower reached with minimal slope.

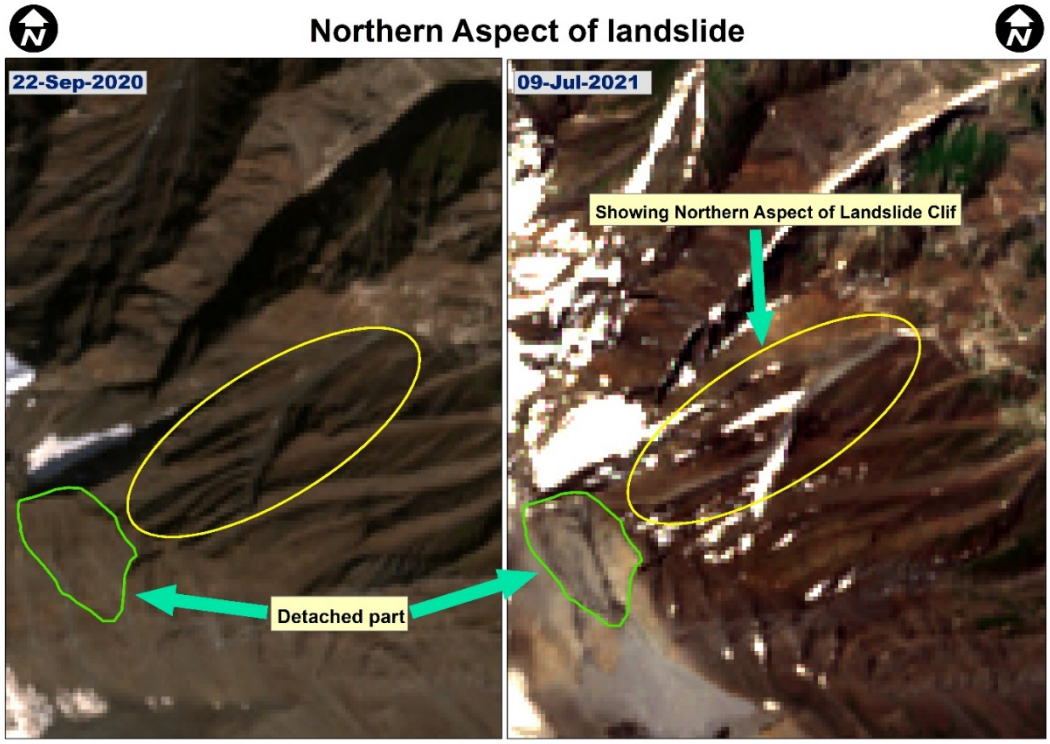

Figure 9: The comparison of both images shows that a small part of slide also flows at the northern aspect of the cliff where landslide occurs (shown in yellow oval) in Naltar Valley. However, this is very small and doesn't disturbs landcover.

Figure 10: The accumulated alluvial fan and damaged forest. The height of the trees in remaining forest provide in insight about the fate of damaged trees and extend of erosion and accumulation debris thickness.

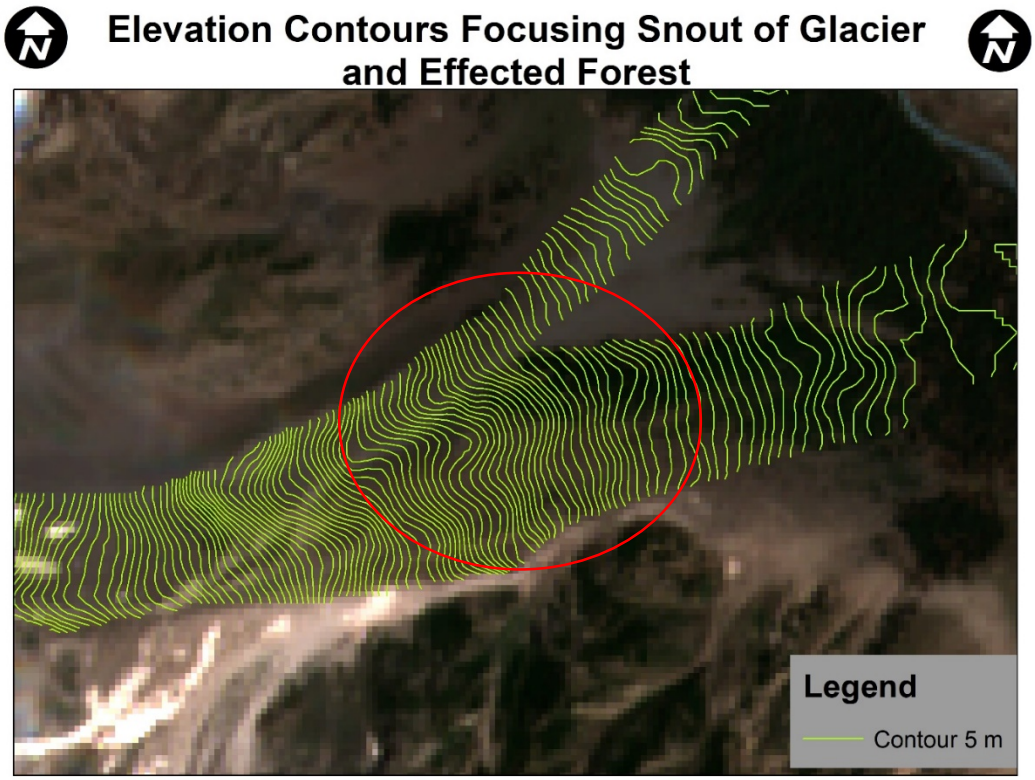

Figure 11: The elevation contour shows that the beginning of forest tree line at upper elevations has an inclined surface from the surroundings. This inclined surface along with forest was eroded as also shown in red circle.

References

Abraham MT, Satyam N, Reddy SKP, Pradhan B. 2021. Runout modeling and calibration of friction parameters of Kurichermala debris flow, India. Landslides. https://doi.org/10.1007/s10346-020-01540-1.

Bouhadad Y, Benhamouche A, Bourenane H, Ouali AA, Chikh M, Guessoum N. 2010. The Laalam (Algeria) damaging landslide triggered by a moderate earthquake (Mw = 5.2). Natural Hazards. https://doi.org/10.1007/s11069-009-9466-0.

Chen W, Li W, Hou E, Bai H, Chai H, Wang D, Cui X, Wang Q. 2015. Application of frequency ratio, statistical index, and index of entropy models and their comparison in landslide susceptibility mapping for the Baozhong Region of Baoji, China. Arabian Journal of Geosciences. https://doi.org/10.1007/s12517-014-1554-0.

Costa JE, Schuster RL. 1988. FORMATION AND FAILURE OF NATURAL DAMS. Bulletin of the Geological Society of America. https://doi.org/10.1130/0016-7606(1988)100<1054:TFAFON>2.3.CO;2.

Dai FC, Lee CF, Deng JH, Tham LG. 2005. The 1786 earthquake-triggered landslide dam and subsequent dam-break flood on the Dadu River, southwestern China. Geomorphology. https://doi.org/10.1016/j.geomorph.2004.08.011.

Dataset: ASF DAAC. 2015. ALOS PALSAR_Radiometric_Terrain_Corrected_low_res; Includes Material © JAXA/METI 2007.

Dawn. 2021. Dawn Newspaper 6th July 2021. https://www.dawn.com/news/1633418.

Dilley M, Chen RS, Deichmann U, Lerner-Lam A, Arnold M, Agwe J, Buys P, Kjekstad O, Lyon B, Yetman G. 2005. Natural disaster hotspots: A global risk analysis. World Bank Disaster Risk Management Series.

Ermini L, Casagli N. 2003. Prediction of the behaviour of landslide dams using a geomorphological dimensionless index. Earth Surface Processes and Landforms. https://doi.org/10.1002/esp.424.

Evans SG, Delaney KB, Hermanns RL, Strom A, Scarascia-Mugnozza G. 2011. The Formation and Behaviour of Natural and Artificial Rockslide Dams; Implications for Engineering Performance and Hazard Management. .

Feizizadeh B, Blaschke T. 2011. Landslide Risk Assessment Based on GIS Multi-Criteria Evaluation : A Case Study in Bostan-Abad County , Iran. Journal of Earth Science and Engeneering.

Fischer L, Purves RS, Huggel C, Noetzli J, Haeberli W. 2012. On the influence of topographic, geological and cryospheric factors on rock avalanches and rockfalls in high-mountain areas. Natural Hazards and Earth System Science. https://doi.org/10.5194/nhess-12-241-2012.

Gardezi H, Xing A, Bilal M, Zhuang Y, Muhammad S, Janjua S. 2022. Preliminary investigation and dynamic analysis of a multiphase ice-rock avalanche on July 5, 2021, in the upper Naltar valley, Gilgit, Pakistan. Landslides. Springer Berlin Heidelberg, 19(2): 451–463. https://doi.org/10.1007/s10346-021-01840-0.

Gong W, Juang CH, Wasowski J. 2021. Geohazards and human settlements: Lessons learned from multiple relocation events in Badong, China – Engineering geologist's perspective. Engineering Geology. https://doi.org/10.1016/j.enggeo.2021.106051.

Gruber S, Fleiner R, Guegan E, Panday P, Schmid MO, Stumm D, Wester P, Zhang Y, Zhao L. 2017. Review article: Inferring permafrost and permafrost thaw in the mountains of the Hindu Kush Himalaya region. Cryosphere. https://doi.org/10.5194/tc-11-81-2017.

Guzzetti F, Peruccacci S, Rossi M, Stark CP. 2008. The rainfall intensity-duration control of shallow landslides and debris flows: An update. Landslides. https://doi.org/10.1007/s10346-007-0112-1.

Hurst MD, Ellis MA, Royse KR, Lee KA, Freeborough K. 2013. Controls on the magnitude-frequency scaling of an inventory of secular landslides. Earth Surface Dynamics. https://doi.org/10.5194/esurf-1-67-2013.

Ischuk AR. 2011. Usoi Rockslide Dam and Lake Sarez, Pamir Mountains, Tajikistan. .

Kazmi., A.H and Jam. M. 1997. Geology and Tectonics. .

Keefer DK. 2002. Investigating landslides caused by earthquakes - A historical review. Surveys in Geophysics. https://doi.org/10.1023/A:1021274710840.

Khan G, Ali S, Xiangke X, Qureshi JA, Ali M, Karim I. 2021. Expansion of Shishper Glacier lake and recent glacier lake outburst flood (GLOF), Gilgit-Baltistan, Pakistan. Environmental Science and Pollution Research. https://doi.org/10.1007/s11356-020-11929-z.

Klose M, Gruber D, Damm B, Gerold G. 2014. Spatial databases and GIS as tools for regional landslide susceptibility modeling. Zeitschrift für Geomorphologie. https://doi.org/10.1127/0372-8854/2013/0119.

Li C, Ma T, Zhu X. 2010. AiNet- and GIS-based regional prediction system for the spatial and temporal probability of rainfall-triggered landslides. Natural Hazards. https://doi.org/10.1007/s11069-009-9351-x.

Mikoš M, Vilímek V, Yin Y, Sassa K. 2017. Advancing Culture of Living with Landslides: Volume 5 Landslides in Different Environments. Advancing Culture of Living with Landslides.

NESPAK. 2010. Dam Break Study of Hunza River near Attabad. Report to the National Disaster Management Authority (NDMA). .

Owen LA, Kamp U, Khattak GA, Harp EL, Keefer DK, Bauer MA. 2008. Landslides triggered by the 8 October 2005 Kashmir earthquake. Geomorphology. https://doi.org/10.1016/j.geomorph.2007.04.007.

Pandey P, Ali SN, Champati Ray PK. 2021. Glacier-Glacial Lake Interactions and Glacial Lake Development in the Central Himalaya, India (1994–2017). Journal of Earth Science. https://doi.org/10.1007/s12583-020-1056-9.

Papathoma-Köhle M, Neuhäuser B, Ratzinger K, Wenzel H, Dominey-Howes D. 2007. Elements at risk as a framework for assessing the vulnerability of communities to landslides. Natural Hazards and Earth System Science. https://doi.org/10.5194/nhess-7-765-2007.

Pradhan B, Mansor S, Pirasteh S, Buchroithner MF. 2011. Landslide hazard and risk analyses at a landslide prone catchment area using statistical based geospatial model. International Journal of Remote Sensing. https://doi.org/10.1080/01431161.2010.484433.

Quincey DJ, Luckman A. 2014. Brief communication: On the magnitude and frequency of Khurdopin glacier surge events. Cryosphere, 8(2): 571–574. https://doi.org/10.5194/tc-8-571-2014.

Saha AK, Gupta RP, Sarkar I, Arora MK, Csaplovics E. 2005. An approach for GIS-based statistical landslide susceptibility zonation-with a case study in the Himalayas. Landslides.

Schneider JF, Gruber FE, Mergili M. 2013. Recent cases and geomorphic evidence of landslide-dammed lakes and related hazards in the mountains of central Asia. Landslide Science and Practice: Risk Assessment, Management and Mitigation.

Shangguan D, Li D, Ding Y, Liu J, Anjum MN, Li Y, Guo W. 2021. Determining the events in a glacial disaster chain at badswat glacier in the karakoram range using remote sensing. Remote Sensing. https://doi.org/10.3390/rs13061165.

Shroder JF. 1998. Slope failure and denudation in the western Himalaya. Geomorphology. https://doi.org/10.1016/S0169-555X(98)00052-X.

Shugar DH, Jacquemart M, Shean D, Bhushan S, Upadhyay K, Sattar A, Schwanghart W, McBride S, de Vries MVW, Mergili M, Emmer A, Deschamps-Berger C, McDonnell M, Bhambri R, Allen S, Berthier E, Carrivick JL, Clague JJ, Dokukin M, Dunning SA, Frey H, Gascoin S, Haritashya UK, Huggel C, Kääb A, Kargel JS, Kavanaugh JL, Lacroix P, Petley D, Rupper S, Azam MF, Cook SJ, Dimri AP, Eriksson M, Farinotti D, Fiddes J, Gnyawali KR, Harrison S, Jha M, Koppes M, Kumar A, Leinss S, Majeed U, Mal S, Muhuri A, Noetzli J, Paul F, Rashid I, Sain K, Steiner J, Ugalde F, Watson CS, Westoby MJ. 2021. A massive rock and ice avalanche caused the 2021 disaster at Chamoli, Indian Himalaya. Science. https://doi.org/10.1126/science.abh4455.

Steiner JF, Kraaijenbrink PDA, Jiduc SG, Immerzeel WW. 2018. Brief communication: The Khurdopin glacier surge revisited - Extreme flow velocities and formation of a dammed lake in 2017. Cryosphere, 95–101.

Tien Bui D, Tuan TA, Klempe H, Pradhan B, Revhaug I. 2016. Spatial prediction models for shallow landslide hazards: a comparative assessment of the efficacy of support vector machines, artificial neural networks, kernel logistic regression, and logistic model tree. Landslides. https://doi.org/10.1007/s10346-015-0557-6.

Tsangaratos P, Ilia I, Hong H, Chen W, Xu C. 2017. Applying Information Theory and GIS-based quantitative methods to produce landslide susceptibility maps in Nancheng County, China. Landslides. https://doi.org/10.1007/s10346-016-0769-4.

Wang LJ, Sawada K, Moriguchi S. 2013. Landslide susceptibility analysis with logistic regression model based on FCM sampling strategy. Computers and Geosciences. https://doi.org/10.1016/j.cageo.2013.04.006.

Wartman J, Montgomery DR, Anderson SA, Keaton JR, Benoît J, dela Chapelle J, Gilbert R. 2016. The 22 March 2014 Oso landslide, Washington, USA. Geomorphology. https://doi.org/10.1016/j.geomorph.2015.10.022.

Wesson RL, Wesson CVK. 1975. Odyssey to Tadzhik: An American family joins a Soviet seismological expedition. U.S. Geological Survey Earthquake Information Bulletin (USGS), 7(1): 8–15.

Wieczorek GF. 1996. Landslide triggering mechanisms. Special Report - National Research Council, Transportation Research Board.

Zhang G, Cai Y, Zheng Z, Zhen J, Liu Y, Huang K. 2016. Integration of the Statistical Index Method and the Analytic Hierarchy Process technique for the assessment of landslide susceptibility in Huizhou, China. Catena. https://doi.org/10.1016/j.catena.2016.03.028.

Zhuang Y, Xing A, Cheng Q, Li D, Zhao C, Xu C. 2020. Characteristics and numerical modeling of a catastrophic loess flow slide triggered by the 2013 Minxian–Zhangxian earthquake in Yongguang village, Minxian, Gansu, China. Bulletin of Engineering Geology and the Environment. https://doi.org/10.1007/s10064-019-01542-x.